Experimental verification of topologically induced vortices inside a billiard

1999 J. Phys. A: Math. Gen. 32 8225

(http://iopscience.iop.org/0305-4470/32/47/302)

J. Phys. A: Math. Gen. **32** (1999) 8225–8230. Printed in the UK PII: S0305-4470(99)07037-7

Experimental verification of topologically induced vortices inside a billiard

P Šeba†, U Kuhl‡, M Barth‡ and H-J Stöckmann‡

† Nuclear Physics Institute, Academy of Sciences, 25068 Řež near Prague, Czech Republic
‡ Fachbereich Physik, Universität Marburg, Renthof 5, D-35032 Marburg, Germany

Received 17 August 1999, in final form 27 September 1999

Abstract. Using flat electromagnetic resonators we experimentally verify the existence of vortices in the Poynting vector describing the energy transport in a rectangular billiard. We show that these vortices appear as a consequence of the nontrivial topological structure of the underlying phase of the electromagnetic field. The results are also relevant for vortices appearing during the quantum transport.

Recent theoretical studies have stressed the importance of topological defects in the structure of the quantum phase. Such defects are responsible for many observable phenomena known mainly to occur in macroscopic quantum systems, for example, superconductors or superfluid helium. However, the phase defects also manifest themselves in the ordinary quantum mechanics. The fact that quantum probability current may exhibit vortices centred at the singular points of the quantum phase has been pointed out already by Dirac [1]. The physical relevance of these vortices was, however, unclear. It has been demonstrated recently [2] that the existence of vortices in the quantum probability flow of charged particles is manifest by a nonzero magnetic dipole moment which leads to measurable effects (at least for a suitable system geometry).

In the case of two-dimensional quantum systems it is possible [2, 3] to identify the configuration space with a region in the complex plane. In such a way, the topology of the related quantum phase can be described with the help of a Riemannian surface. The multivaluedness of the phase (which is defined as modulo 2π) can be expressed in terms of various Riemannian sheets and the topological defects can be identified with branching points and cuts on the Riemannian surface. To be more explicit, let us write the probability current density $\vec{j}(\vec{r})$:

$$\vec{j}(\vec{r}) = \frac{\hbar}{m}\mathrm{Im}\,(\psi^*(\vec{r})\vec{\nabla}\psi(\vec{r})) \tag{1}$$

and the wavefunction ψ as

$$\psi = \sqrt{\rho}\mathrm{e}^{\mathrm{i}S} \tag{2}$$

where $\rho = |\psi|^2$ is the probability density and S denotes the phase. It is clear that the phase S cannot be defined on the nodal points of the wavefunction ψ, which represent singularities of S. The nontrivial topological structure of the phase leads to the appearance of vortices in the related probability current. To see this we insert (2) into (1) and get

$$\vec{j}(\vec{r}) = \frac{\hbar}{m}\rho(\vec{r})\vec{\nabla}S(\vec{r}). \tag{3}$$

0305-4470/99/478225+06$30.00

The current $\vec{j}$ can be understood as a flow of the probability density ρ with a velocity $\vec{v} = (\hbar/m)\vec{\nabla}S$. The vorticity of $\vec{v}$ evaluated along a closed curve Γ gives [4]

$$\int_\Gamma \vec{v}\,\mathrm{d}\vec{l} = \frac{\hbar}{m}\delta S = 2\pi\frac{\hbar}{m}n \qquad n = 0, \pm 1, \pm 2, \ldots \tag{4}$$

where δS is the phase change when winding once around the curve. The wavefunction (2) must be single-valued, which means that the difference δS can only be equal to a multiple of 2π.

If the phase S does not have a branching point inside Γ, the difference equals to zero and the vorticity nullifies. If, on the other hand, Γ encircles a branching point of S, the vorticity of the velocity field $\vec{v}$ is not zero. In this situation the corresponding probability current exhibits a vortex centred at the nodal point.

It has been argued in [2] that the vortices of the quantum probability current produce nonzero magnetic dipole moments. To measure this effect is, however—due to the low values of the magnetic dipole—extremely complicated and, even for the most optimistic situation, is only on the border of today's achievable accuracy. There is, however, another experimental possibility to verify the existence of the vortices which is based on the fact that electromagnetic fields inside flat electromagnetic resonators fulfil the same equations of motion as the quantum particle. This fact has been successfully used for experimental verification of the spectral properties [5–7] and the wavefunctions [8, 9] of chaotic two-dimensional quantum billiards.

The transport of electromagnetic energy through the resonator is described by the Poynting vector

$$\vec{P}(\vec{r}, t) = \frac{c}{4\pi}(\vec{E} \times \vec{H}). \tag{5}$$

Entering with ansatz $\vec{E}(\vec{r}, t) = \mathrm{Re}\,(\vec{E}(\vec{r})\mathrm{e}^{-\mathrm{i}\omega t})$, $\vec{H}(\vec{r}, t) = \mathrm{Re}\,(\vec{H}(\vec{r})\mathrm{e}^{-\mathrm{i}\omega t})$ into the Maxwell equations, (5) reads

$$\vec{P}(\vec{r}, t) = \frac{c}{4\pi k}(\mathrm{Re}\,(\vec{E}) \times (\vec{\nabla} \times \mathrm{Im}\,\vec{E})) \tag{6}$$

with k being the wavevector of the field $\vec{E}(\vec{r})$. For quasi-two-dimensional resonators this formula reduces to

$$\vec{P}(\vec{r}, t) = \frac{c}{4\pi k}(E_R \cos(\omega t) + E_I \sin(\omega t)) \cdot \vec{\nabla}(E_I \cos(\omega t) - E_R \sin(\omega t)) \tag{7}$$

where E_R and E_I are real and imaginary parts of the z component of $\vec{E}(\vec{r})$, respectively. Taking only the stationary part of $\vec{P}(\vec{r}, t)$, we arrive at

$$\langle\vec{P}(\vec{r}, t)\rangle = \frac{c}{8\pi k}\mathrm{Im}\,(E_z^*(\vec{r})\vec{\nabla}E_z(\vec{r})). \tag{8}$$

This is in complete analogy with equation (3), where the stationary part of the Poynting vector replaces the probability current density, and the z component of the electric field strength replaces $\Psi(\vec{r})$.

It is a well established theoretical concept that defects in phase topology are responsible for vortex phenomena in various quantum systems (for instance, the appearance of Abrikosov vortices in superfluid helium [10]). They have also been observed as dislocations in wave trains of ultrasonic echoes [11]. More recently, the defects were seen experimentally in optical systems and interpreted as angular momenta of light [12, 13].

However, detailed experimental verification has still been missing. The point is that one can usually measure the probability/energy transport in the system and verify the existence of the vortices, but the topology of the phase itself escapes a direct observation. The experiment described below allows a direct measurement of $E_z(\vec{r})$ as a function of position, including its phase, and constructs the related Riemannian surface.

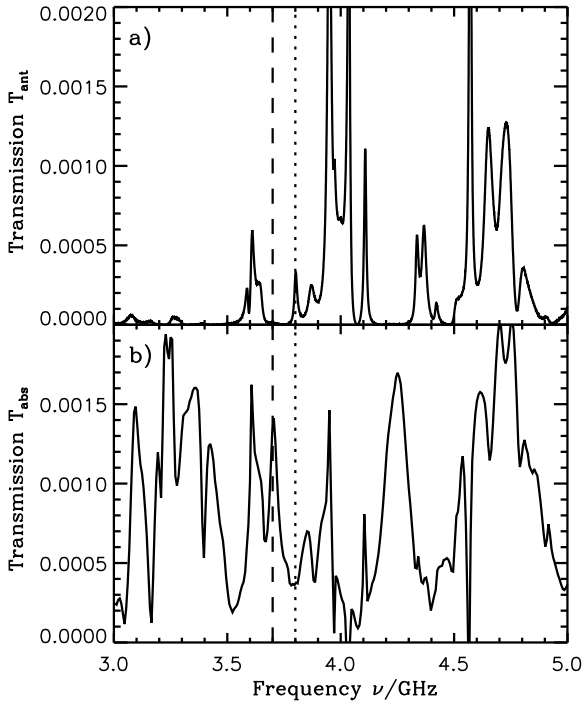

Figure 1. (*a*) Transmission $T_{\rm ant} = |t_{\rm ant}|^2$ from the entrance antenna to the probing antenna. (*b*) Transmission $T_{\rm abs}$ from the entrance antenna to the absorber.

The experimental set-up is a further development of an apparatus described previously in [8, 14]. The cavity has a rectangular shape with dimensions $l_x = 34$ cm, $l_y = 24$ cm where the entrance antenna is positioned at $x = 8$ cm, $y = -2$ cm. The electromagnetic energy has been transported from this antenna to a circular absorber with radius $r = 2.5$ cm placed at $x = -6$ cm, $y = 5$ cm (see figure 2). The position of the upper plate supporting the probing antenna is varied by means of step motors in the x- and y-directions with a stepsize of 5 mm. The transmission amplitude $t_{\rm ant}$ between entrance and probing antenna has been measured, including the phase, by means of a Wiltron 360B vector network analyser. The influence of the cables, connectors, antenna wires etc on the transmission has been determined in a separate measurement and is not included in the figures presented below.

It has been shown in [14] that $t_{\rm ant}$ is proportional to the electric field strength at the position $\vec{r}$ of the probing antenna. In figure 1(*a*) the transmission $T_{\rm ant} = |t_{\rm ant}|^2$ is shown for the position ($x = -10$ cm, $y = 2$ cm) of the probing antenna. From the measured electric field strength $E_z(\vec{r})$ the energy flow is determined by means of equation (8).

The intensity of the electromagnetic field inside the resonator depends on its frequency. For certain frequencies there is an enhanced transport of the electromagnetic energy from the antenna to the absorber. The transmission from the entrance antenna to the absorber, normalized to the total energy within the resonator, is plotted in figure 1(*b*) as a function of frequency. The figure has been obtained by integrating the flow through the surface of a square with a sidelength of 8 cm, covering the absorber (a square has been chosen, since the data have been taken on a square lattice: the shape of the area is irrelevant because of Gauss's law). Figure 2 shows the Poynting vector in the resonator for the frequency marked by a dashed line in figure 1. The vortices are clearly visible. We have also evaluated the

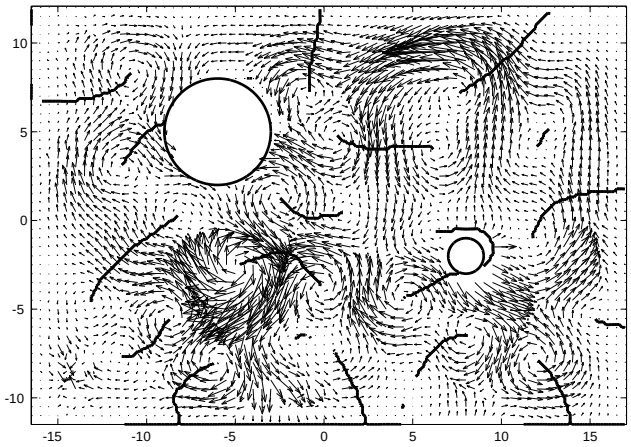

Figure 2. Flow of the electromagnetic energy from the entrance antenna (small circle) to the absorber (large circle) at frequency $v = 3.7$ GHz (marked by the dashed line in figure 1). At the solid curves the wavefunction has acquired a phase of 2π upon encircling a vortex. These curves correspond to cuts in the Riemannian surfaces (see figure 3).

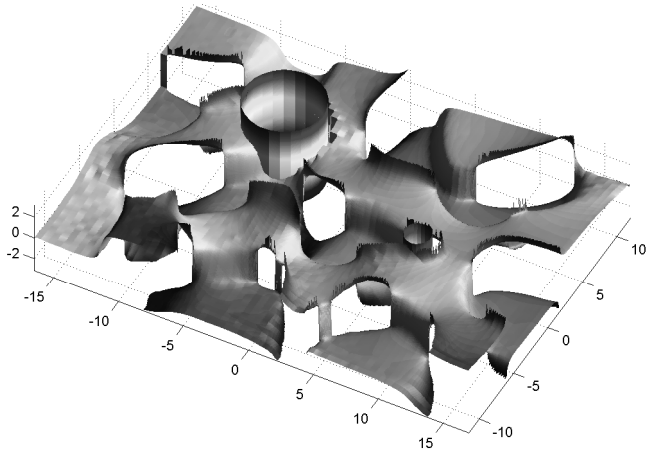

Figure 3. Three-dimensional view of the phase of the flow pattern shown in figure 2.

corresponding phase of the related electromagnetic field and plotted its cuts into the same plot (thick curves). One can see—in full agreement with the theory—that the cuts start at the centre of the vortices. This supports the theoretical finding that a vortex winds around a branching point of the related Riemannian surface of the phase. All observed vortices have the vortex number $n = \pm 1$. Vortices with higher vortex numbers n have not been observed in the experiment. The phase of the field is plotted in figure 3. The positions of the entrance antenna and the absorber are marked by inserted cylinders. The complicated structure of the corresponding Riemannian surface together with the branching points and the cuts is clearly visible. Similar pictures can also be plotted for other frequencies. Although the position and number of vortices changes, the basic structure and the relation between the vortices and the phase topology remains unchanged.

Figure 1(*b*) shows that there are a number of frequencies where the flow to the absorber

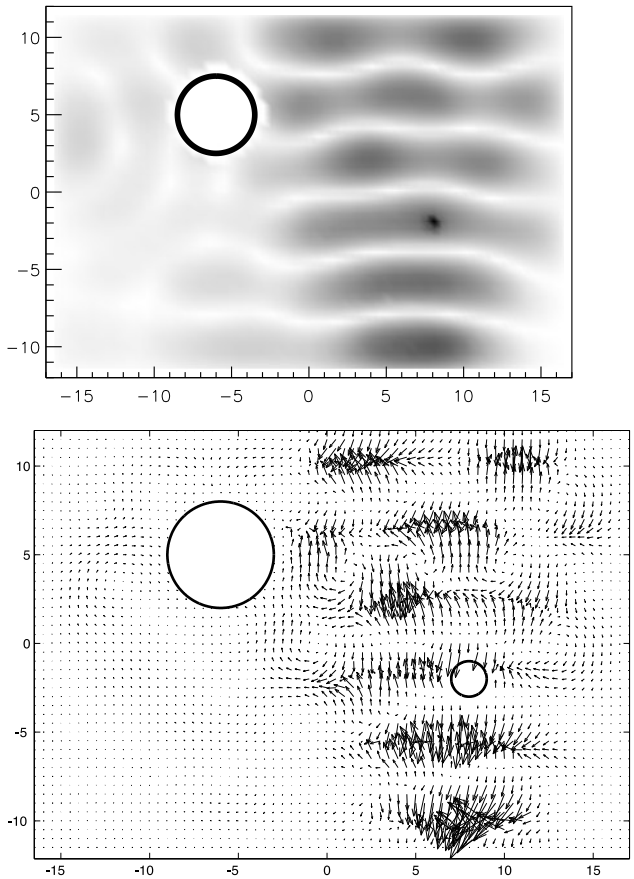

Figure 4. (*a*) Greyscale plot of $|E|^2$ at the frequency $\nu = 3.8$ GHz (marked by a dotted line in figure 1). At this frequency there is no flow to the absorber. (*b*) Flow pattern at the same frequency. At the points of large field strength a maximal flow to the probing antenna is observed.

is close to zero. This means, however, that at these frequencies there must be a node line at the surface of the absorber, or, in other words, these frequencies must correspond to eigenfrequencies of the Sinai billiard obtained by replacing the absorber surface by a reflecting wall. This interpretation is corroborated by figure 4(*a*) showing a map of $|E|^2$ in a greyscale at a frequency corresponding to the dotted line in figure 1. The figure clearly exhibits a bouncing ball eigenfunction of the Sinai billiard. Figure 4(*b*) shows the corresponding flow pattern. Since at this frequency the flow to the absorber is suppressed, the otherwise negligible leak to the probing antenna becomes dominant (the absorption in the walls is too small to become observable in the flow pattern). The leak flow is maximized at the points of large field strengths as expected. The same findings can be obtained from a comparison of figures 1(*a*) and (*b*): the relative transmission from the entrance to the probing antenna shows a maximum whenever the transmission to the absorber exhibits a minimum.

To conclude, let us mention that the particular setting of the measured system is not substantial for the underlying physics. The rectangular shape of the resonator and the circular shape of the absorber have been chosen due to technical reasons. We expect that similar phenomena will also be observed in different configurations, provided there is a flow of

electromagnetic energy inside the system and the system is not integrable (transport through ideal integrable waveguides is not accompanied by phase defects). It must be stressed, however, that the existence of phase defects and related vortices is of pure wave origin and is not related to the underlying classical dynamics. In such a way it cannot be seen as a signature of 'quantum chaos'.

Acknowledgments

This work has been partially supported by the Theoretical Physics Foundation at Slemeno, by the grant GAAV 1048804 from the Czech Academy of Sciences and by the Deutsche Forschungsgemeinschaft via the Sonderforschungsbereich 'Nichtlineare Dynamik'.

References

[1] Dirac P 1931 *Proc. R. Soc.* A **133** 60
[2] Exner P *et al* 1998 *Phys. Rev. Lett.* **80** 1710
[3] Berggren K and Ji Z-L 1993 *Phys. Rev.* B **47** 6390
[4] Hirschfelder J 1977 *J. Chem. Phys.* **67** 5477
[5] Stöckmann H-J and Stein J 1990 *Phys. Rev. Lett.* **64** 2215
[6] Gräf H-D *et al* 1992 *Phys. Rev. Lett.* **69** 1296
[7] So P, Anlage S, Ott E and Oerter R 1995 *Phys. Rev. Lett.* **74** 2662
[8] Stein J and Stöckmann H-J 1992 *Phys. Rev. Lett.* **68** 2867
[9] Sridhar S 1991 *Phys. Rev. Lett.* **67** 785
[10] Lifschitz E M and Pitaevskij L P 1978 *Statisticeskaya Fyzika* (Moscow: Nauka)
[11] Nye J F and Berry M V 1974 *Proc. R. Soc.* A **336** 165
[12] Arecchi F T *et al* 1991 *Phys. Rev. Lett.* **67** 3749
[13] Dholakia K *et al* 1996 *Phys. Rev.* A **54** R3742
[14] Stein J, Stöckmann H-J and Stoffregen U 1995 *Phys. Rev. Lett.* **75** 53